

# Analysis of Mechanical Properties of Three-Dimensionally Braided Composite

Okuwobi Idowu Paul

Graduate Student, Mechanical and Electrical Engineering Department, Nanjing University of Aeronautics and Astronautics, Nanjing, China 210016

**Abstract**— This research uses the Finite Element Analysis software ANSYS to build a four step 3D-braided composite micromechanical model and analyses its properties. With the assumption that the fibre bundle is transversely isotropic and the matrix is isotropic, the macroscopic elastic constants of 3D-braided composites were simulated, and the elastic constants versus the braiding angles and fibre volume fraction were analysed. The presence of reinforcement along the thickness direction in three-dimensionally braided composites, increases the through thickness stiffness and strength properties, more so the three-dimensionally preforms can be manufactured with numerous complex architecture variations to meet the needs of specific application.

Among the advantages of this technique (FEM) is simplicity and the ability to model and study the response of complex shapes subjected to complex loads applied at any boundary of the design model.

## I. INTRODUCTION

Three dimensionally woven textiles are not only beautiful, they also have the potential to change the way aircraft and other complex structures are built. Recently both Airbus and Boeing, the two leading aircraft manufacturers, have in their strive to reduce structural weight, dramatically increased the use of fibre reinforced composite materials in their new aircraft. The development can be exemplified by the Boeing 787 Dreamliner which is the first commercial aircraft with both composite wings and fuselage, for which the combined weight of the composite parts account for 50% of the structural weight [1]. This trend marks a shift from using composite materials in only secondary structures (i.e. radar domes and control surfaces etc.) to also use composites in load bearing primary structures. However, the increased use of composite materials is associated with increased manufacturing costs [2]. Today the state of the art manufacturing method for primary aircraft structures made of carbon fibre reinforced plastics (CFRP), is prepreg layup. The mechanical properties of composites made from prepreg are characterized by high in-plane stiffness and strength and lower out-of-plane stiffness and strength. According to Naik and Ganesh [3] the majority of primary loads in aircraft structures are in-plane, and hence motivate the use of prepreg laminates. The fuselage is an

example of such development. However, in parts such as stiffeners and stringers not all loads are in-plane, making the prepreg laminate with its low out-of-plane lamina stiffness and strength less suitable. Composite materials with better through thickness mechanical properties are thus desired to substitute today's metal parts where such loads occur.

## II. BRAIDING

The dimensions of the braided structures are used as criteria for categorizing braiding. A braided structure having two braided yarn systems with or without a third laid-in yarn is considered as two-dimensional braided structure involving three or more systems of braided yarns to form an integrally braided structure is three dimensional braided processes.

### A. Three-Dimensional Braiding Process

The recently developed three-dimensional braiding techniques have greatly improved the design of performs for advanced composites. Different three different dimensional processes have be built, such as horn-gear braiding process, two step braiding process, four step braiding process, multi-step process.

- Four-Step Braiding Process

The four step braiding process involves four distinct Cartesian motions of groups of yarns termed rows and columns. For a given step, alternate rows (or columns) are shifted a prescribed distance relative to each other. The next step involves the alternate shifting of the columns (or rows) a prescribed distance. The third and fourth steps involve simply the reverse shifting sequence of the first and second steps, respectively. A complete set of four steps is called a machine cycle as shown in Fig.01. It should be noted that after one machine cycle the rows and columns have returned to their original positions. The braid pattern shown is of the 1×1 variety, so termed because the relation between the shifting distance of the rows and columns is one to one. Other braid patterns (i.e., 1×3, 1×5, vect.) are possible but they requires different machine bed configurations and a specialized machine. Row and column braiding yarn carries of the type depicted in Fig.01 may be used to fabricate performs of rectangular cross sections such as T-beam, I-beam, and box beam.

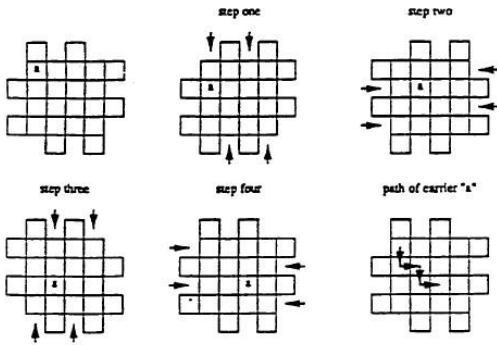


Fig.01 The four-step braiding process

cell is divided into two forms which are denoted by type A and type B (as shown in fig.02, fig.03)

There are three kinds of single cell in the material arrangement which is displayed in fig.04.

Here is the internal unit cell geometry parameter of the cell as shown in fig.05:

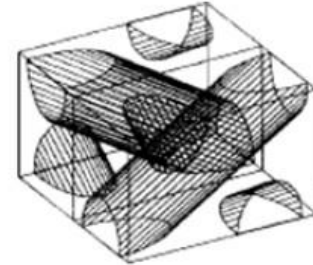


Fig.02 Type A body cell

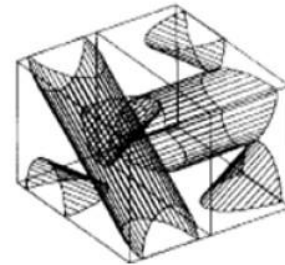


Fig.03 Type B body cell

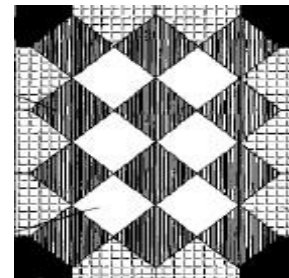


Fig.04 Cell arrangement

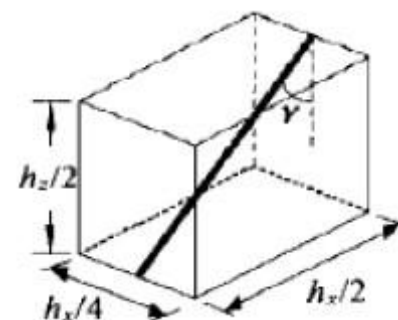


Fig.05 Unit cell geometry parameter

### III. MODELLING AND STIFFENESS ANALYSIS

#### A. Basic Assumption

The fibre bundle passes along six surface unit cell body in diagonal direction, and the geometric fibre bundles is simply regarded as line. Four step braided composites for three-dimensional cell body geometry assumption will be analysed in this work. This model does not completely reflect the fibre bundle structure and the interleaving mode, which in the actual three-dimensional braided composite material structure can completely be reflected. The cell body, fibre bundles and the gap are all in the same level of scale in terms of characteristic. So in terms of geometric concepts or the mechanics meaning general fibre bundles is simplified as a line is not suitable.

The combination of previous work as well as my own understanding in the establishment of braided composite material model as brought about the following assumptions:

1. Fibre bundle has a circular cross section, and cross section shapes along the fibre axis direction remains the same. So in this paper, the cylinder shaped fibre bundle is transversely isotropic.
2. All have the same geometric properties of fibre bundle.
3. Substrate is a cube model, and isotropic.
4. The fibres and the matrix is bonded, no relative displacement.
5. As a result of the braiding process retraction movement of the tension, the preforms internal fibre beam bending was caused.

#### B. Model Selection

This paper takes a cylinder instead of fibre bundles; a cuboids representing matrix material. Due to boundary and corner cell bodies in the total volume of the percentage, this paper focuses on the analysis of body of single cell and the establishment of finite element model, in order to simulate three-dimensional braided composite performance. Single

Therefore,  
 $\gamma = \arctan (h_x/h_z)$  ..... (1.1)

$V = 2\pi r^2/ h_x^2 \cos \gamma$  ..... (1.2)

IV. MATERIALS AND PARAMETERS

Putative braided yarn after curing was put into the composite material rod, whose cross section is circular, and cross sectional area is the same as the composite material with a fixed value. As a result of this, it resulted in a transversely isotropic with a unidirectional composite material bar with a high rigidity of elastic constants.

$$E_1 = E_{f1} V_{f1} + E_m V_m \dots\dots\dots (1.3)$$

$$E_2 = E_3 = E_m / [1 - V_{f1} (1 - E_m / E_{f2})] \dots\dots\dots (1.4)$$

$$G_{12} = G_{13} = G_m / [1 - V_{f1} (1 - G_m / G_{f12})] \dots\dots\dots (1.5)$$

$$G_{23} = G_m / [1 - V_{f1} (1 - G_m / G_{f23})] \dots\dots\dots (1.6)$$

$$v_{12} = v_{13} = v_{f12} V_{f1} + v_m V_m \dots\dots\dots (1.7)$$

$$v_{21} = v_{12} E_1 / E_2 \dots\dots\dots (1.8)$$

$$v_{23} = E_2 / 2G_{23} - 1 \dots\dots\dots (1.9)$$

In the formula above,

- E- Elastic modulus,
- G - Shear modulus,
- V - Poisson's ratio
- M – Matrix angle
- F – Fibre
- V<sub>m</sub> – Matrix volume fraction
- V<sub>f</sub> – Fibre volume fraction

This paper assume V<sub>m</sub> =0, V<sub>f</sub> = 1 which means that the model used in this paper identified the fibre bundle as only fibre without been mixed with the matrix. For clarity and proper calculation of needed data for the needed materials, below is the table for all parameters used in this model as shown in table -01.

Table – 01 Material Parameters

|              | E <sub>1</sub> /<br>GPa | E <sub>2</sub> /<br>GPa | G <sub>12</sub> /<br>GPa | G <sub>23</sub> /<br>GPa | v <sub>12</sub> | v <sub>23</sub> |
|--------------|-------------------------|-------------------------|--------------------------|--------------------------|-----------------|-----------------|
| Carbon fibre | 220                     | 13.8                    | 9.0                      | 4.8                      | 0.20            | 0.25            |
| Epoxy resin  | 4.5                     |                         |                          |                          | 0.34            | 0.34            |

V. MODEL

This project work using finite element model created 8 different types of three dimensional braided composite materials, and there geometric parameters are shown below in table - 02:

Table – 02 Geometry Parameter of the model

| No.                | 1    | 2    | 3    | 4    | 5    | 6    | 7    | 8    |
|--------------------|------|------|------|------|------|------|------|------|
| Braiding angle (°) | 50   | 40   | 30   | 25   | 25   | 25   | 25   | 20   |
| Fiber vol. ratio   | 0.45 | 0.45 | 0.45 | 0.45 | 0.50 | 0.35 | 0.40 | 0.45 |

From the geometry parameter, γ=50°, V= 0.45, the following figure represent the matrix model -fig.06 , fibre model -fig.07, and the single cell model -fig.08.

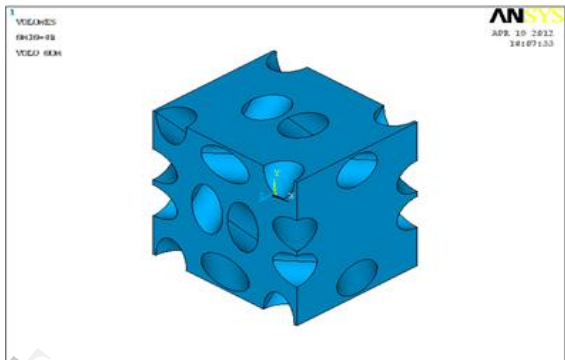


Fig.06 Matrix model when γ=50°, V<sub>f</sub> = 0.45

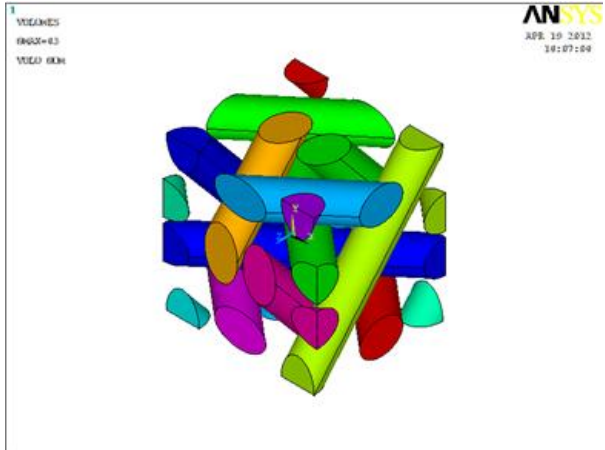


Fig.07 Fibre model when γ=50°, V<sub>f</sub> = 0.45

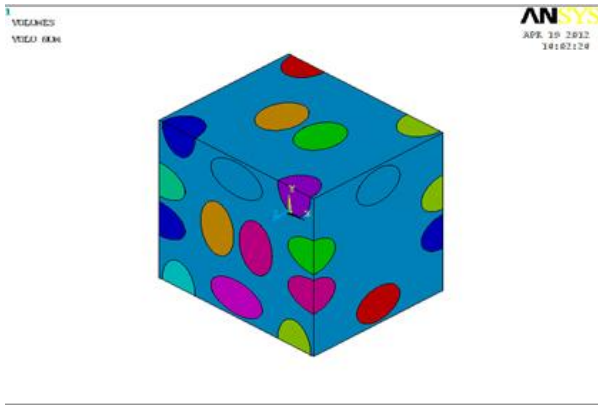


Fig.08 Single cell model when  $\gamma=50^\circ$ ,  $V_f = 0.45$

VI. GRID DIVISION

In accordance with our assumption, using eight nodes, and each node has 3 degrees of freedom of the SOLID-45 unit, the bundle of fibres and matrix are grid. These units in general constitutive equation of discrete produces discrete results:

$$[C] \{D\} = \{R\} \dots\dots\dots (1.10)$$

In the formula, [C] represent the element stiffness matrix, {D} for node displacement, {R} the unit node load. In equation (1.10) by Integration, the result is:

$$[C] \{D\} = \{R\} \dots\dots\dots (1.11)$$

In the formula above, [C] is the structural stiffness matrix, {D} for nodal displacements, and {R} is the structure node load. Below is the fibre and single cell combined finite element mesh when  $\gamma=50^\circ$  and  $V_f=0.45$  (Fig.09).

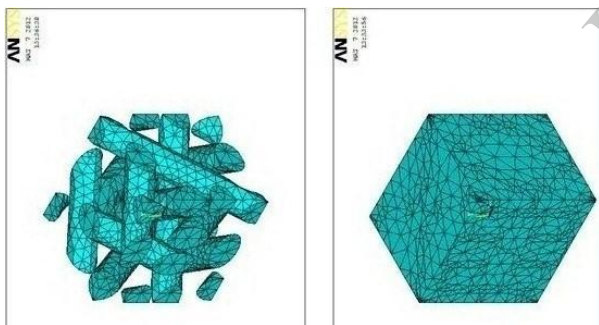


Fig.09 Fibre and single cell finite element mesh when  $\gamma= 50$  and  $V_f= 0.45$

Due to the fibre local material coordinates and global coordinates inconsistency, to create a uniform view of the fibre material the coordinate transformation method was used. The effective elastic properties of the local coordinate system of the material were converted to the overall. The effective elastic properties in the coordinate system were then substituted into the unit (Solid-45) attribute to be calculated, so that the entire specimen could be known and calculated. The stiffness matrix of the fibre bundle can be expressed as:

$$[C_Y] = [T] [C_Y'] [T]^T \dots\dots\dots (1.12)$$

Where,  $[C_Y]$  is the stiffness of the fiber bundles in the global coordinate system matrix,  $[C_Y']$  is the stiffness matrix of the fiber bundles in the local coordinate system, which can be expressed as:

$$[C_Y'] = [S_Y']^{-1} = \begin{bmatrix} \frac{1}{E_1} & -\frac{\nu_{12}}{E_1} & -\frac{\nu_{13}}{E_1} & 0 & 0 & 0 \\ -\frac{\nu_{12}}{E_1} & \frac{1}{E_2} & -\frac{\nu_{23}}{E_2} & 0 & 0 & 0 \\ -\frac{\nu_{13}}{E_1} & -\frac{\nu_{23}}{E_2} & \frac{1}{E_2} & 0 & 0 & 0 \\ 0 & 0 & 0 & \frac{1}{G_{23}} & 0 & 0 \\ 0 & 0 & 0 & 0 & \frac{1}{G_{12}} & 0 \\ 0 & 0 & 0 & 0 & 0 & \frac{1}{G_{12}} \end{bmatrix}^{-1}$$

The coordinate transformation matrix [T]:

$$[T] = \begin{bmatrix} l_1^2 & m_1^2 & n_1^2 & 2m_1n_1 & 2n_1l_1 & 2l_1m_1 \\ l_2^2 & m_2^2 & n_2^2 & 2m_2n_2 & 2n_2l_2 & 2l_2m_2 \\ l_3^2 & m_3^2 & n_3^2 & 2m_3n_3 & 2n_3l_3 & 2l_3m_3 \\ l_2l_3 & m_2m_3 & n_2n_3 & m_2n_3 + m_3n_2 & n_2l_3 + n_3l_2 & l_2m_3 + l_3m_2 \\ l_3l_1 & m_3m_1 & n_3n_1 & m_3n_1 + m_1n_3 & n_3l_1 + n_1l_3 & l_3m_1 + l_1m_3 \\ l_1l_2 & m_1m_2 & n_1n_2 & m_1n_2 + m_2n_1 & n_1l_2 + n_2l_1 & l_1m_2 + l_2m_1 \end{bmatrix}$$

$$l_1 = \cos\gamma\cos\theta, \quad l_2 = \cos\gamma\sin\theta, \quad l_3 = \sin\gamma; \\ m_1 = \sin\gamma, \quad m_2 = \cos\theta, \quad m_3 = 0; \\ n_1 = \sin\gamma\cos\theta, \quad n_2 = \sin\gamma\sin\theta, \quad n_3 = \cos\gamma;$$

Where  $\gamma$  is the unit cell of braided angle,  $\theta$  is the angle of the fibre bundles in the XY plane projection of the Y-axis. According to the equation 1.12, we can get the stiffness matrix  $[C_Y]$ , inverse flexibility matrix [SY], and then obtain the fibre bundles in the global coordinate. The engineering relationship between elastic constants and the flexibility matrix is shown below:

$$E_{fz} = 1/S_{11}, \quad E_{fy} = 1/S_{22}, \quad E_{fx} = 1/S_{33} \dots\dots\dots (1.13)$$

$$\nu_{fyz} = -S_{21}/S_{11}, \quad \nu_{fzx} = -S_{31}/S_{11}, \quad \nu_{fxy} = S_{32}/S_{22} \dots\dots\dots (1.14)$$

$$G_{fxy} = 1/S_{44}, \quad G_{fyz} = 1/S_{55}, \quad G_{fzx} = 1/S_{66} \dots\dots\dots (1.15)$$

VII. ELASTIC CONSTANT CALCULATION

For different analysis on the objects, various loads were imposed on the model; the displacement field of the model can be calculated. The average strain field can be obtained by the load of the average stress of the model, and the macroscopic elastic constants of the model as a whole can be obtained by the stress and strain. Zero displacement constraints imposed at the bottom of the model and the upper part exert a uniform pressure; while the rest of the plane left with free boundary conditions, the Z-direction is the displacement distribution (see fig.10).

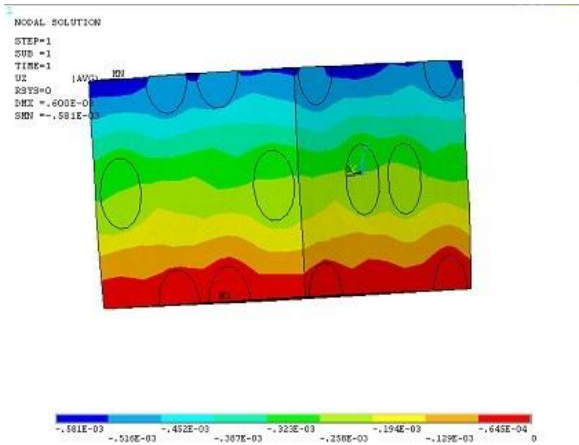


Fig.10 Displacement distribution in Z-direction

At  $Z = 2$  the model at the top in force displacement distribution can be obtained by the weighted average of the surface displacement from  $Z = 2$  to  $z = 0.5485 \times 10^{-3}$ mm, the model can be calculated in accordance with the following formulas in the direction of the elastic modulus:

$$E_z = (F/A) / (\Delta z/h) = 16.13 \text{ GPa}$$

According to  $X = 2.2$ , the mean displacement  $\Delta x$  can be calculated as  $\Delta v_{xz}$ :

$$v_{xz} = (\Delta x/h) / (\Delta z/h) = 0.27$$

Average displacement  $\Delta y$  according to  $Y = 2.2$  surface, it can be calculated as  $v_{yz}$ :

$$v_{yz} = (\Delta y/h) / (\Delta z/h) = 0.35$$

Using different geometric parameters on the braided composite model to obtain the elastic constant which are different based on the geometric parameters used. This method was repeated for 8 times with varying parameters in order to obtain the data below. Table - 03 shows the detail.

Table – 02 Geometric parameters under varying elastic constants of braided composites

|            | 1     | 2     | 3     | 4     | 5     | 6     | 7     | 8     |
|------------|-------|-------|-------|-------|-------|-------|-------|-------|
| $E_z$ /GPa | 16.14 | 24.98 | 37.78 | 62.74 | 47.70 | 50.85 | 34.41 | 31.64 |
| $E_x$ /GPa | 17.51 | 14.73 | 12.51 | 10.14 | 11.57 | 12.75 | 10.37 | 7.31  |
| $E_y$ /GPa | 17.74 | 14.57 | 12.62 | 10.77 | 11.42 | 12.55 | 10.63 | 7.56  |
| $v_{xy}$   | 0.31  | 0.28  | 0.24  | 0.29  | 0.27  | 0.24  | 0.29  | 0.32  |
| $v_{yz}$   | 0.33  | 0.53  | 0.67  | 0.51  | 0.62  | 0.67  | 0.54  | 0.50  |
| $v_{zx}$   | 0.29  | 0.56  | 0.60  | 0.49  | 0.58  | 0.68  | 0.53  | 0.49  |

### VIII. RESULT ANALYSIS

According to the result obtained, the graph of change in elastic constants with changing in fibre volume ratio, and changing in braiding angle can be plotted. In this paper, the graph of elastic constants with the braiding angle graph is represented in fig.11 and fig.12 at  $V = 0.45$  and  $\gamma$

$= 25^\circ$ , while the graph of elastic constants with fibre volume ratio is represented in fig.13 and fig.14.

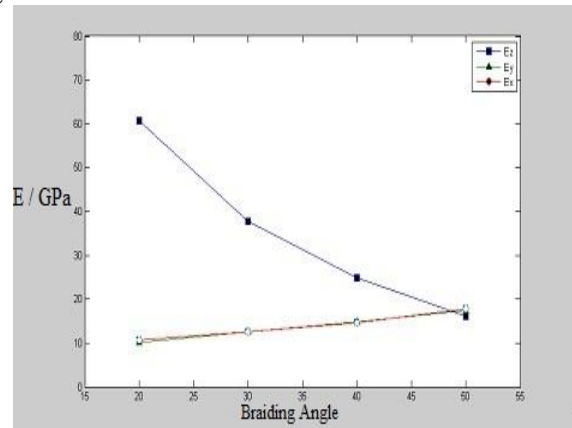


Fig.11 Elastic constant E against braiding angle  $\gamma$  at constant  $V_f = 0.45$

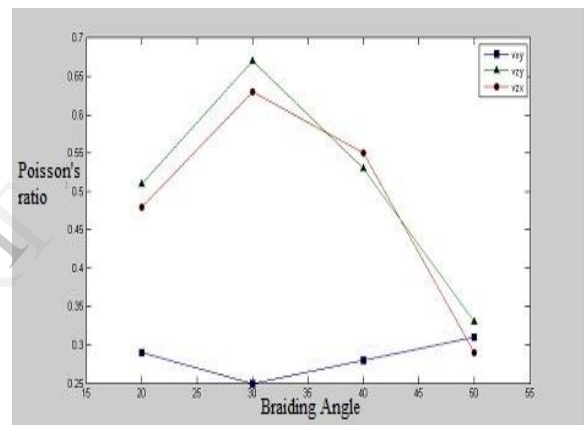


Fig.12 Poisson's ratio against braiding angle  $\gamma$  at constant  $V_f = 0.45$

The elastic modulus  $E_z$  against the braiding angle can be seen from fig.11 from the graph, it is discovered that the elastic constants of braided composites decreases as the braiding/ weaving angle increases significantly. While  $E_x$  and  $E_y$  increases slightly as weaving angle increases. As shown in fig.12 as the weaving angle increases  $v_{ZY}$  and  $v_{ZX}$  increases sharply for the first increase in the weaving angle and started decreasing for the consequence increases in the weaving angle. While  $v_{XY}$  decreases for the first increase in the weaving angle, and keep increasing for the consequence increase in the weaving angle. The trend  $v_{ZY}$  and  $v_{ZX}$  is basically the same, which is as large as the weaving angle, by the influence of the spatial position of the fibre bundles in the z direction the deformation increases, but the x, y direction of the deformation decreases gradually. Braiding angle reaches a certain angle, which corresponds to the maximum deformation ratio in the z-direction. The corresponding x, y directions represent the minimum deformation, which make  $v_{XY}$  first decreases and then increases.

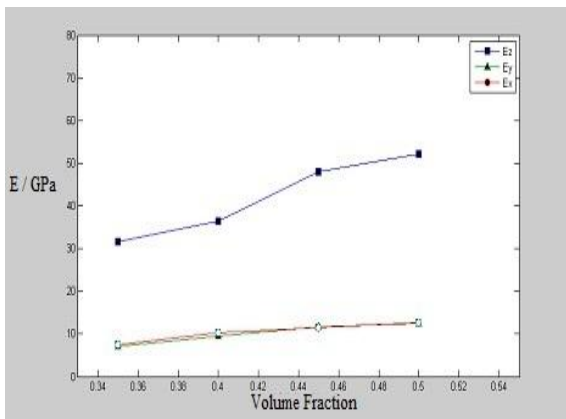


Fig.13 Elastic constant E against fiber volume fraction curve at  $\gamma = 25^\circ$

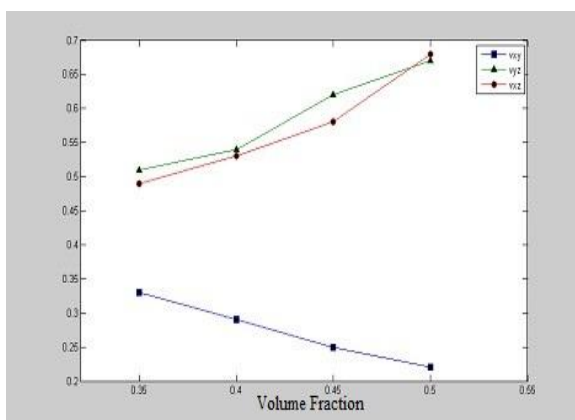


Fig.14 Poisson's ratio against Fiber volume fraction at  $\gamma = 25^\circ$

From fig.13 it can be seen that as fiber volume fraction increases, modulus of elasticity is gradually increasing as well, with the rate of increase  $E_z$ ,  $E_x$  and  $E_y$ . Also from fig.14  $\nu_{xz}$  and  $\nu_{yz}$  similar increasing trend,  $\nu_{xy}$  showed a downward trend. This is because with the increase of fiber volume fraction, the effective performance of the material as a whole has been enhanced. In X, Y, and Z-direction deformation were reduced, while the z direction enhances the effect of strength,  $\nu_{xz}$  and  $\nu_{yz}$  have a corresponding increase, and  $\nu_{xy}$  reduces. This study found that both woven angular size and the effective performance of the materials have similar trends with the changes in the fiber volume fraction, but decreases gradually with an increase in the weave angle trend.

In the finite element analysis, the structure are divided into many small units, each unit provides a finite number of degrees of freedom, but in fact these small units are infinite degrees of freedom, which means that we increase the deformation capacity of the unit artificial restrictions, that is, an increase of the stiffness and the stiffness of the entire

object is increased, therefore, finite element calculations is too large; but at the same time, a large number of studies have shown that the surface cells and the corner cell of the braided composite materials modulus of elasticity is much larger than the single cell. This article uses cell combination to simulate the calculation of the stiffness of 3D braided composites, so the result is so small. Finally, we must recognize that three dimensional 3D braided composites are a complex in nature including their stiffness, strength and mechanical properties etc. The volume fraction and the braiding angle and yarn orientation, as well as the matrix and the yarn are all interface binding functions. The spatial orientation of the yarn is subjected to fabric parameters, such as squeezing of the degree of inter-yarn linear density (yarn size) in the preform, the number of impact etc. These parameters were obtained based on a lot of experiments done in order to establish more reasonable, close to the actual model, the effective use of finite element methods and existing software. Thus, the mechanical properties of 3D braided composites using computer simulation were done.

## IX. CONCLUSION

From the result generated from this paper work, it could be concluded that the elastic modulus varies with the braiding angle of the 3D-braided composite. Also when the braiding angle increases the elastic modulus decreases significantly.  $E_z$  decreases as braiding angle increases, while  $E_x$  and  $E_y$  increases slightly as braiding angle increases. The Poisson's ratio of both  $\nu_{xz}$  and  $\nu_{yz}$  in XY and YZ direction increases with an increase in the fiber volume fraction, while  $\nu_{xy}$  in the XY direction decreases as the fiber volume fraction increases.

## X. REFERENCES

- [1] Avva V. S, et al, Through-the-Thickness Tension Strength of 3-D Braided Composites [J]. Journal of Composite Materials, 1966, 30(1): pp.51-68
- [2] Du Guang-Wu, Tsu-Wei Chou, Analysis of Three-Dimensional Textile Preforms for Multidirectional Reinforcement of Composites [J]. Journal of Materials Science, 1966, 26: pp.3438-3446.
- [3] Zeng T, Wu Lz, Guo LC, Ma Li [J]. Material Science and Engineering, 2004, 1: pp144~151. [2] Jones, C.D., A.B. Smith, and E.F. Roberts, *Book Title*, Publisher, Location, Date.
- [4] Weller R.D, AYPEx: A New Method of Composite Reinforcement Braiding [C]. United States, NASA Conference Publication, 1985.
- [5] F. K. Koin, T.W Chou and F. K Ko, Textile Structural Composites [M]. 2<sup>nd</sup>, United States, Elsevier Publishers, 1989: pp. 120-150.
- [6] C. C Chamis, Simplified Composite Micromechanics Equations for Hygral, Thermal, and Mechanical Properties [J]. SAMPE Quarterly, 1984, 40: pp. 14-23.
- [7] Kostar T.D, T-W. Chou, Process Simulation and Fabrication of Advanced Multi-Step Three-Dimensional Braided Preforms [J]. Journal of Materials Science, 1994, 29: pp.2159-2167.
- [8] Hamada Hiroyuki, et al, CAE in Integrated Braided Composite [J]. Science and Engineering of Composite Material, 1995, (2): pp.109-120.
- [9] Pastore, C.M and F.K.KO, A processing Science model for Three Dimensional Braiding [J]. SAMPE Quarterly, 1988, 19(4): pp22-28.